OPEN ACCESS

Formation of a non-magnetic metallic iron nitride layer on bcc Fe(100)

New Journal of Physics
The open-access journal for physics

Formation of a non-magnetic metallic iron nitride layer on bcc Fe(100)

C Navío[1,2,5], M J Capitán[3], J Álvarez[1,2], R Miranda[1,2,4] and F Yndurain[1,2]

[1] Departamento de Física de la Materia Condensada, Universidad Autónoma de Madrid, Cantoblanco, 28049 Madrid, Spain
[2] Instituto Nicolás Cabrera, Universidad Autónoma de Madrid, Cantoblanco, 28049 Madrid, Spain
[3] Instituto de Estructura de la Materia—CSIC, c/Serrano 119, 28006 Madrid, Spain
[4] Instituto Madrileno de Estudios Avanzados en Nanociencia (IMDEA), Spain
E-mail: cristina.navio@uam.es

New Journal of Physics **12** (2010) 073004 (13pp)
Received 28 January 2010
Published 1 July 2010
Online at http://www.njp.org/
doi:10.1088/1367-2630/12/7/073004

Abstract. We report the formation of a stable iron nitride thin film following the exposition of an Fe(001) single crystal to atomic N plasma produced by means of a radio-frequency (rf) discharge source. The obtained phase, enabled by N-atomic diffusion into the iron matrix, has been characterized using spectroscopical and structural techniques. The comparison of the experimental results with first-principles calculations sheds light on the formed structure stability. The result is the formation of a metallic non-magnetic protective coating film on the iron substrate with a zinc blende (ZB) structure (γ''-FeN). The formed film has high oxidation resistance, metallic character, non-magnetic ground state and good epitaxial growth. Thermal treatment of the iron nitride film shows that, at around 700 K, the FeN is decomposed, resulting in bcc Fe as a consequence of the high diffusivity of N in Fe.

[5] Author to whom any correspondence should be addressed.

Contents

1. Introduction

The behavior and properties of nitrogen on metals has been studied extensively for many years, owing to its relevance in catalysis processes, corrosion, etc. Recently, due to the magnetic properties of some iron–nitrogen compounds, there has been increasing interest in the behavior of nitrogen in Fe. Atomic and molecular diffusion in crystals plays a fundamental role in the final properties of the material. In the case of bcc Fe, the diffusion of most common contaminants has been reviewed in [1]. The interaction of atomic and molecular nitrogen with different iron surfaces has been studied by several authors, in particular by Bozso *et al* [2], Scholten *et al* [3] and Ertl *et al* [4]. The possibility of the formation of a surface iron nitride has been considered by other authors [5, 6].

The N/α-Fe system has been investigated in great detail by several groups. Here, we will focus our attention on the growth of a two-dimensional surface nitride layer on Fe(001). So far the formation of N/Fe surface compounds has been experimentally accessible via three different approaches: (a) the segregation of interstitially bulk dissolved nitrogen towards the Fe(001) surface [7]; (b) thermal decomposition of NH_3 on the Fe(100) surface; and (c) the dissociative adsorption of N_2 [8]. The segregation route (a) needs a high temperature to promote the nitrogen atom mobility and its diffusion towards the surface (800 °C) and therefore the simultaneous desorption of molecular nitrogen [9] takes place. The alternative approach based on the NH_3 (b) requires temperatures above 400 °C at which the decomposition of the ammonia molecule takes place. The hydrogen resulting from the ammonia decomposition desorbs, leaving only nitrogen at the surface. At this temperature, thermodynamically stable Fe_4N bulk nitride [8] is formed. In the dissociative adsorption of N_2, case (c), the rate-limiting step is the dissociation of the nitrogen molecule at the surface, together with the entropic barrier. This means that there is an energy barrier (activation energy), which grows with the nitrogen coverage, of a few tens of eV per molecule. Thus, the atomic diffusion of nitrogen into the bulk is highly dependent on the dissociation step. Nevertheless, some of the absorbed nitrogen atoms diffuse into the ferritic bulk, as has been demonstrated by means of isotope exchange experiments [2].

In this work, in order to avoid the aforementioned drawbacks of pre-existing growth methods, we propose the use of a nitrogen plasma source to study the atomic diffusion of nitrogen into an α-Fe(001) single crystal and the formation of an iron–nitrogen compound. This method precludes the molecular dissociation barrier or the use of high temperature compared to the other aforementioned methods. These experimental studies will allow us to elucidate

whether thin films with nitrogen atoms in subsurface positions might be thermodynamically stable at intermediate-low temperature conditions or whether they could form stable compounds other than the Fe_4N (thermodynamically stable at temperatures above 400 °C). Nevertheless, it has already been established that the Fe-N-atomic plasma codeposition at room temperature forms a γ''-FeN zinc blende (ZB) structure [10].

2. Experimental methods and theoretical simulation

FeN(001) films were grown at 300 K in an ultrahigh vacuum (UHV) chamber with a base pressure of 3×10^{-10} mbar, by exposing an Fe(001) single crystal to a beam of atomic nitrogen produced by a radio-frequency (rf) plasma discharge source [11] with a nitrogen pressure of 1×10^{-6} mbar in the vacuum chamber. As the gas source in the rf plasma source, nitrogen was used with an internal pressure of 10^{-2} mbar [12]. The efficiency of production of atomic N was 15% in the experimental conditions used.

The chemical characterization, the stoichiometry and the thickness of the grown films were determined *in situ* by x-ray photoelectron spectroscopy (XPS; $h\nu$ (Mg K_α) = 1253.6 eV), using a Hemispherical Analyzer Leybold–Heraeus (LHS10) to detect the ejected electrons. The density of states (DOS) of the valence band was measured with ultraviolet photoelectron spectroscopy (UPS) at 21.2 eV (He-I) and 40.8 eV (He-II). The sample was annealed to study the thermal stability of the formed phase. The annealing temperature was measured by comparing the readings of a calibrated platinum resistor (PT100) and a chromel-alumel thermocouple attached to the sample. At high temperatures, an optical pyrometer was also used.

The structural characterization has been performed by means of both *in situ* low energy electron diffraction (LEED) and *ex situ* x-ray diffraction (XRD). The XRD measurement was made using a six-circle diffractometer with optimized geometry for surface analysis at the W1.1 beamline of the Hasylab synchrotron at DESY, using a wavelength of 1.393 Å.

The experimental results were complemented by first-principles theoretical calculations performed in the context of density functional theory [13] using the SIESTA [14] method (see below).

3. Results

3.1. Experimental results

We present the changes produced in the Fe(001) bcc surface after exposing to N-atomic plasma at room temperature. The XPS N 1s signal, shown in figure 1, clearly increases in intensity after the substrate exposition to the N plasma. The N 1s spectra (figure 1(b)) change with respect to the Fe(001) with a half monolayer of nitrogen at the surface forming a $c(2 \times 2)$ reconstruction [2, 5, 15] used as reference (fitted with the dashed component of figure 1(a)), not only for intensity but also for peak position and shape. The N 1s core level peak of the formed compound is located at a binding energy of 398.25 eV. This value must be compared to 397.80 eV, which is characteristic of the Fe–N bond, strongly heteropolar with charge transferred from Fe → N, intrinsic to the nitrogen segregated to the surface [16, 17]. The peak shift is evidence of the interaction of the N-atoms with the iron substrate, and the high peak intensity indicates the large incorporation of N-atoms to the iron substrate. The peak is fitted

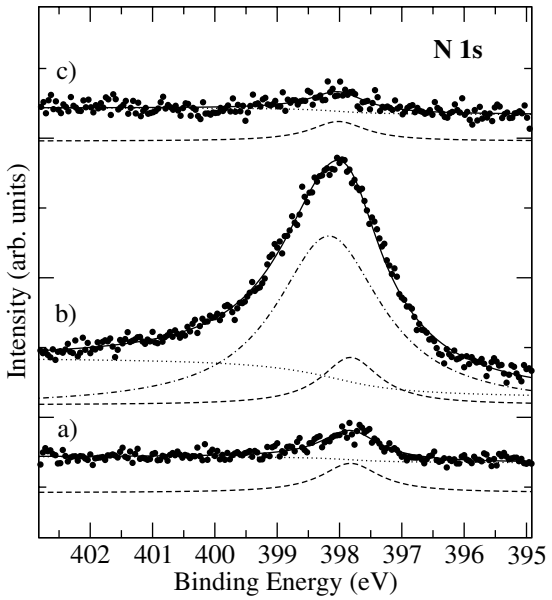

Figure 1. N 1s peaks for (a) the Fe(001) single crystal with 0.5 ML of N; (b) as-grown N-atomic plasma onto Fe(001) at room temperature; and (c) after annealing at 680 K. The dashed curve is the fit for the surface N $c(2 \times 2)$ component. The dot-dashed curve corresponds to the fit for the bulk nitrogen component. The dotted line is the Shirley integral background used in the fit.

with two components. The first corresponds to surface nitrogen (dashed line in figure 1(b)), while the second component corresponds to bulk nitrogen (dot-dashed line in figure 1(b)).

The interaction of the diffused N-atoms with the iron matrix is also reflected in the Fe 2p core level peaks, shown in figure 2. In this figure, the Fe 2p spectra of the iron substrate exposed for 10 min to a plasma of nitrogen at room temperature (figure 2(b)) are compared with the initial state, which corresponds to an Fe(001) single crystal with 0.5 ML (monolayer) of N segregated from substrate annealing during the preparation. The latter is used as a reference due to its well-known $c(2 \times 2)$ reconstruction and electronic structure [2, 5, 15, 16]. As can be seen, the Fe 2p peaks (figure 2(b)) are not only displaced in energy but also change in width and asymmetry with respect to the reference (figure 2(a)). The resulting peak can be fitted with two components: one that is characteristic of pure Fe (with parameters obtained from the reference, figure 2(a)), and a second component that is characteristic of a formed iron nitride compound. The intensity attenuation of the pure Fe component after the exposition of the iron sample to the nitrogen plasma (dashed line in figure 2(b)) indicates that an iron nitride layer of 32 Å depth has been formed. The as-grown Fe/N atomic ratio was 1.2 ± 0.3, determined by quantitative XPS using the iron-reacted component of the fit and the N 1s core level peak, indicating that the formed compound has an $Fe_{1.2}N$ stoichiometry. Thus, when the Fe(001) is exposed to atomic N at room temperature, this N diffuses into the crystal through several monolayers (between 20 and 40 Å, depending on the plasma source parameters), forming an iron nitride 1 : 1 overlayer.

UPS experiments complete the photoemission study of this system, giving information about the valence band. In figure 3, we can see the He I spectra corresponding to (a) a half monolayer of N on Fe(001), used as reference, which is characterized by an intense peak at 5 eV

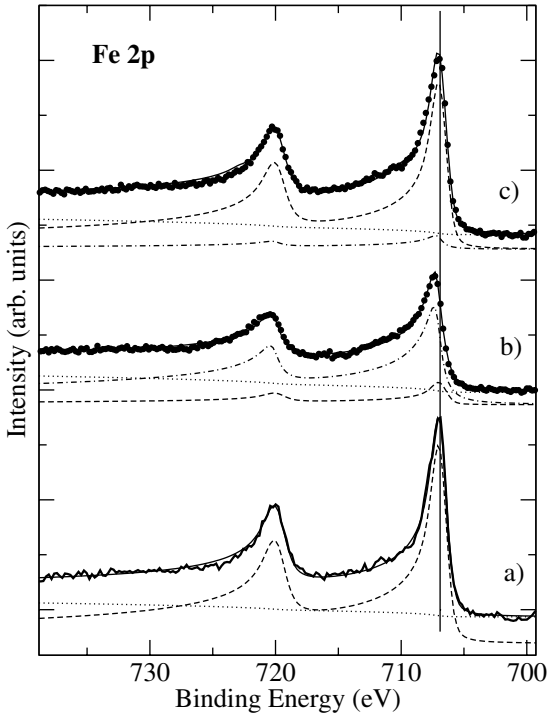

Figure 2. Fe 2p peaks for (a) the Fe(001) single crystal with 0.5 ML of N; (b) as-grown N-atomic plasma onto Fe(001) at room temperature; and (c) after annealing at 680 K. The dashed curve corresponds to the bulk iron component. The dot-dashed curve corresponds to the fit for the nitrogen bonded iron component. The dotted line corresponds to the integral Shirley background used in the fit.

below the Fermi level; and (b) the UPS spectra of the result of exposing an Fe(001) single crystal to an N-atom plasma at room temperature. These spectra correspond to a metallic compound (non-zero DOS at the Fermi level). The high background intensity in the spectra indicates the importance of inelastic collisions of the photoemitted electrons going towards the surface [18]. These spectra are almost identical to the characteristic of the FeN with a ZB structure formed by codepositing Fe and N atoms at room temperature [10] (figure 3(c)). The Fe 2p and N 1s photoemission peaks resulting from the exposure of the Fe(001) surface to the N-plasma at room temperature agree with the formation of this iron nitride with ZB structure (noted as γ''-FeN) in the peak shape, the peak position and the relative Fe/N intensity.

The structural characterization has been performed by means of both *in situ* LEED under UHV conditions and *ex situ* XRD. The LEED pattern (figure 4) for the nitrided sample measured at an electron beam energy of 23.4 eV (figure 4(b)) is compared to the $c(2 \times 2)$ reconstruction of N on Fe(001) measured at 60 eV (figure 4(a)). In both cases the resulting pattern is mainly led by the lattice created by the presence of nitrogen atoms [2], [4]–[6], [15, 19, 20]. The lattice ratio between both patterns agrees with a γ''-FeN structure.

The *ex situ* XRD pattern measured along the substrate (001) direction is shown in figure 5. In this pattern, only the Fe(002) peak of the substrate and the γ''-FeN(002) can be observed. These results confirm that, by exposing the Fe(001) substrate to an N-atomic plasma, an epitaxial and well crystallized in the z-direction γ''-FeN film is formed. The peak width of

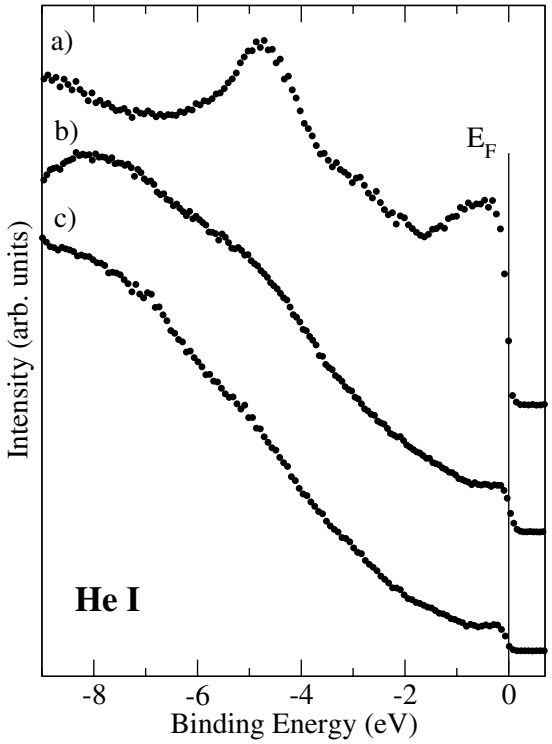

Figure 3. UPS He I spectra for (a) the Fe(001) single crystal with 0.5 ML of N; (b) as-grown N-atomic plasma onto Fe(001) at room temperature; and (c) a reference of a 32 Å-thick film of γ''-FeN grown at room temperature on Cu(001) [10].

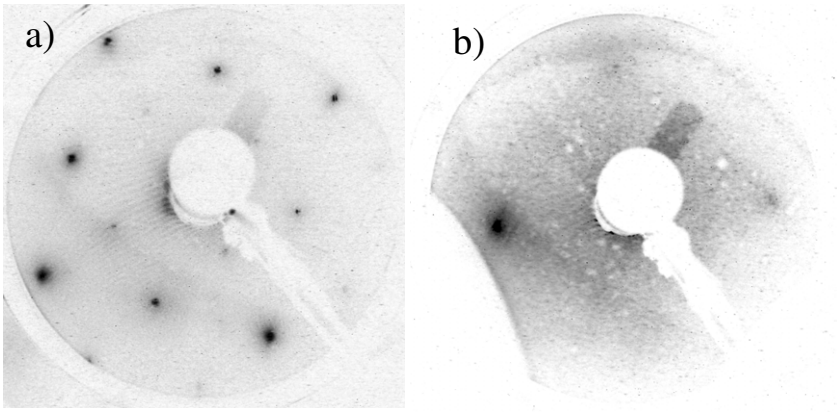

Figure 4. LEED patterns for (a) the Fe(001) single crystal with 0.5 ML of N; (b) as-grown nitrided Fe(001). LEED pattern (a) was taken at 60 eV and (b) was taken at 23.4 eV.

the γ''-FeN(002) Bragg reflection recorded in the XRD pattern gives an average grain size in the z-direction of 32 Å. The theoretical fit of the signal rising up at low angle (from 0° to 10°) of figure 5 (reflectivity peaks) gives us a film thickness of 30 ± 3 Å with a relatively sharp interphase.

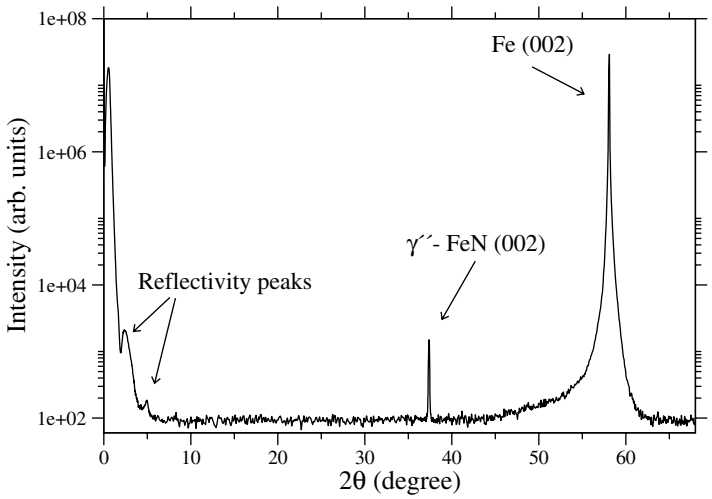

Figure 5. XRD pattern for the as-grown nitrided Fe(001) crystal at room temperature.

The iron nitride compound with ZB structure (γ''-FeN(001)) can be formed by codeposition of Fe and N atoms while keeping a Cu(001) substrate at room temperature. On the other hand, codeposition of Fe and N keeping the substrate at temperatures above 670 K results in the formation of the γ'-Fe_4N phase [10, 16]. However, in the present case, the iron substrate acts as an iron source. Thus the iron is exposed to a plasma of atomic nitrogen, resulting in the 'nitridation' of the substrate, forming the γ''-FeN(001) phase.

The growth of a surface layer of γ''-FeN(001) fcc phase (lattice constant $a = \gamma''_{\mathrm{FeN}} = 4.307$ Å) at the Fe(001) bcc ($a_{\mathrm{Fe}} = 2.866$ Å) substrate is possible only if the former grows rotated 45° with respect to the iron lattice ($a_{\mathrm{Fe}} \times \sqrt{2} = 4.053$ Å). The *in-plane* misfit between both phases is around 6%, which is within the acceptance for epitaxial growth. The incorporation of the nitrogen atoms into the interstitial positions in the Fe matrix implies a significant expansion of the Fe-planes along the out-of-plane direction ((001) direction).

Although the coexistence of this ZB phase with its iso-stoichiometric NaCl-type phase has been reported, our experimental data for the codeposition do not indicate the presence of this phase [10]. Furthermore, in the present case, the misfit of the iron lattice with the lattice parameter of this phase ($a\gamma'''_{\mathrm{FeN}} = 4.50$ Å), 11%, inhibits its formation [21]–[25].

3.2. Theoretical calculations

The first stage of the nitrogen adsorption on Fe(001) has been theoretically studied by several authors, although all these studies start from N_2 molecules. The dissociative chemisorption of nitrogen on the iron surface becomes the rate-limiting step [2, 35, 36]. In these studies it is necessary to take into account that the nitrogen molecule has a high dissociation energy and that the sticking probability of a molecule on single-crystal planes is extremely low, although the activation barriers are not high (i.e. $E_A = 15\,\mathrm{kJ\,mol^{-1}}$ for N_2/Fe(001)) or even negligible (for the N_2/Fe(111) case). The latter aspect must be interpreted in terms of the special orientation of molecules to undergo dissociative adsorption and the lateral interactions between adsorbed nitrogen atoms. The first term (N_2 dissociation) is neglected in our case because we start

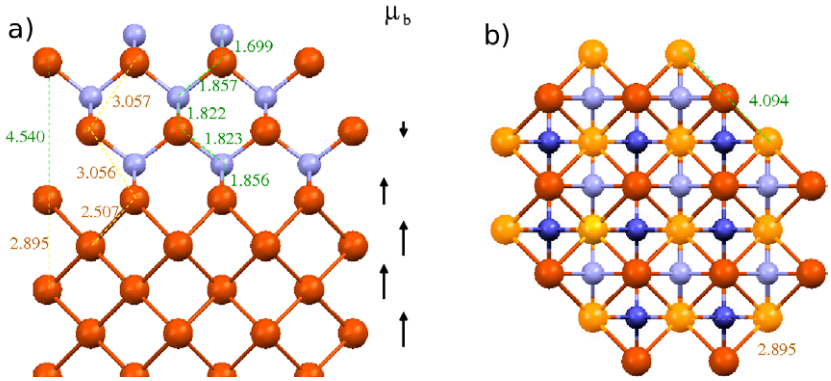

Figure 6. Calculated stable structure for the γ''-FeN growth on bcc Fe: the N atoms diffuse towards inner Fe planes occupying the tetrahedric positions. Fe and N atoms are indicated in red and blue, respectively. The most characteristic atomic distances are indicated in angstroms. Panels (a) and (b) are the side and top views, respectively. At the surface the N atoms are only slightly shifted up and towards the Fe–Fe edge with respect to the $p(1 \times 1)$N structure. The arrows in the right-hand side of panel (a) indicate the magnetic moments of the different Fe layers. The size of the arrows is proportional to the magnitude of the magnetic moment (see table 1).

from an N-atomic plasma. Nevertheless, even including the high dissociative term, it has been demonstrated, by means of isotope exchange experiments, that the adsorption of N_2 on Fe(001) single-crystal surfaces produces the diffusion of some of the adsorbed N atoms into the ferritic bulk [2].

For a complete analysis of the structure stability of the FeN film grown on the Fe(001) substrate, we have performed a first-principles calculation using SIESTA code [14]. For the exchange correlation potential we adopt a generalized gradients approximation [26]. The norm-conserving pseudopotentials used follow the Troullier–Martins scheme [27] in the non-local form proposed by Kleinman and Bylander [28] and with partial core corrections. We first calculated pure γ''-FeN and the bcc Fe structures to be compared with the resulting FeN layer growth model. For the pure crystalline structures we obtained an equilibrium lattice constant of 4.250 and 2.895 Å for γ''-FeN and bcc Fe, respectively, which are within 1.3% of the experimental ones, which are a good test for the calculation method used. We considered a slab of five FeN layers and eight Fe(001) layers. In the calculations, all the atomic positions were relaxed until the residual forces on each atom were less than 0.01 eV $Å^{-1}$. The resulting structure of γ''-FeN layer grown on Fe(001) substrate was stable and is shown in figure 6. This epitaxial growth implies an in-plane contraction (4.094 Å in the structure top view, figure 6(b)) of the γ''-FeN structure with respect to the pure phase, and an out-of-plane expansion shown in the Fe–Fe z-distance (4.540 Å in the structure lateral view, figure 6(a)). These values indicate that the in-plane contraction, induced by matching with the Fe bcc substrate structure in the γ''-FeN layer, is relaxed along the z-layer direction.

The formation of the γ''-FeN phase implies a large adsorption-induced relaxation along the iron (001) planes in order to accommodate the N atoms in the Fe bulk. Although, in principle, the expansion can seem very high, it is known that this phenomenon happens to the same

Table 1. Magnetic moment and spin–resolved charge at the different atoms near the FeN–Fe interface. Atoms are labeled from the outermost N layer towards the Fe bulk. Spin up, spin down and total charge are given in electron units.

Atom-layer index	Magnetic moment (μ_B)	Spin up (e^-)	Spin down (e^-)	Q_{Total} (e^-)
N-1	−0.007	2.537	2.544	5.081
Fe-2	0.062	3.936	3.874	7.810
N-3	0.004	2.659	2.655	5.314
Fe-4	−0.463	3.586	4.049	7.635
N-5	−0.059	2.634	2.693	5.327
Fe-6	1.753	4.782	3.029	7.811
Fe-7	2.626	5.313	2.687	8.000
Fe-8	2.435	5.229	2.794	8.023
Fe-9	2.485	5.23	2.745	7.975
Fe-10	2.451	5.208	2.757	7.965
Fe-11	2.535	5.226	2.691	7.917

extent, which can be observed in other similar systems, such as the oxidation of the Fe(001) bcc [29]–[31]. In the Fe(001) bcc oxidation, the O-atoms enter the iron and adopt a cubic FeO structure. This iron oxide phase has a lattice parameter ($a_{FeO} = 4.290$ Å) that is very close to that corresponding to the γ''-FeN phase. In the Fe(001) oxidation, it has been established that the formed FeO(001) has a very low misfit in the *in-plane* directions and a large relaxation in the z-direction, even in the very initial stages of the oxidation process [29]–[31].

At half-monolayer coverage, the adsorption site at the Fe(001) surface is the symmetrically and highly coordinated hollow (fourfold) site forming the $c(2 \times 2)$ reconstruction for both nitrogen [2, 19] and oxygen [31]–[34] absorption. But the ($p(1 \times 1)$) reconstruction observed for one-oxygen monolayer absorbed [31]–[34] has not been experimentally observed for the one-nitrogen monolayer. This has been explained by the fact that the experiments were performed at low pressure, where the large negative value of the chemical potential for N in the gas phase (experiments were made with N_2) hinders its formation [35]. However, the calculated stable surface (top view, figure 6(b)) approaches a $p(1 \times 1)$ reconstruction at the surface, but with the N-atoms slightly out of the Fe-outermost layer plane. Although Pick *et al* [35] concluded that the absorption energy in tetrahedric sites with a $p(1 \times 1)$ overlayer is slightly unfavorable with respect to the octahedrical sites, the fact that the formed phase is thermodynamically stable and has an adequate lateral lattice parameter with respect to the iron bulk allows this phase transformation.

The theoretical calculations also indicate that the magnetic moment at the Fe atoms (see table 1) changes from a large value (of the order of $2.5\mu_B$ from layer Fe-7 to Fe-11 in table 1) and with ferromagnetic coupling in the Fe-bcc substrate (values in red) to paramagnetic (i.e. equal spin population) in the formed FeN layer (layer Fe-2 in table 1). However, due to the sharp magnetic change, the first Fe-atomic layer of the FeN–Fe interphase shows a very interesting antiferromagnetic coupling (layer Fe-4). The lack of strong deformations at the interface is also reflected in the calculated DOS shown in figure 7. The DOS at the inner layers of the FeN slab is rather similar to the DOS of an FeN single crystal (see figure 7 (b)). This is in agreement

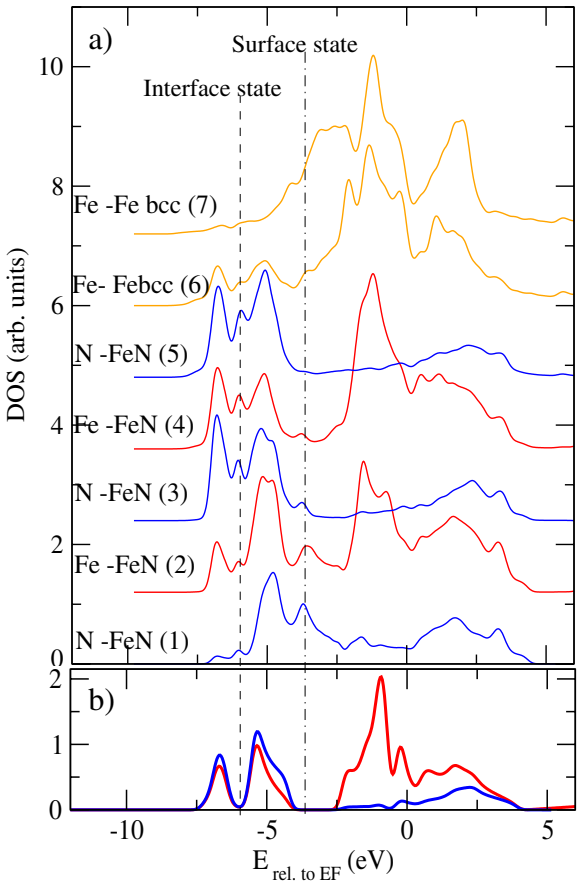

Figure 7. Calculated total DOSs for the Fe–FeN system. In (a) the DOSs at the different layers of the slab shown in figure 6 are shown. In (b) the DOS of bulk FeN in the ZB structure is shown. Blue and red lines are nitrogen and iron atomic planes, respectively, for an FeN film. Orange lines correspond to Fe-bcc atomic layers. Vertical broken lines indicate the surface and interface state energies in the Fe–FeN system.

with the fact that the measured UPS spectrum for the pure ZB FeN phase (figure 3(c)) is similar to the FeN growth on the Fe substrate one (figure 3(b)). We have found, in the calculation, the existence of a surface state localized at the outermost N layer and an interface state localized at the interface between iron and FeN (marked by green and light blue in figure 7, respectively). These new states could possibly be measured by angular resolved photoemission.

In this direction, previous calculations indicate that the formed γ''-FeN (001)/Fe (001) interphase is geometrically, chemically and magnetically sharp, opening up interesting technological applications.

3.3. Thermal stability

After annealing the formed γ''-FeN/Fe (001) layer at 680 K for 10 min, the LEED shows a different pattern, which corresponds to a $c(2 \times 2)$ reconstruction of N on Fe(001) (which is identical to figure 4(a)). This thermal evolution differs with respect to annealing a thin

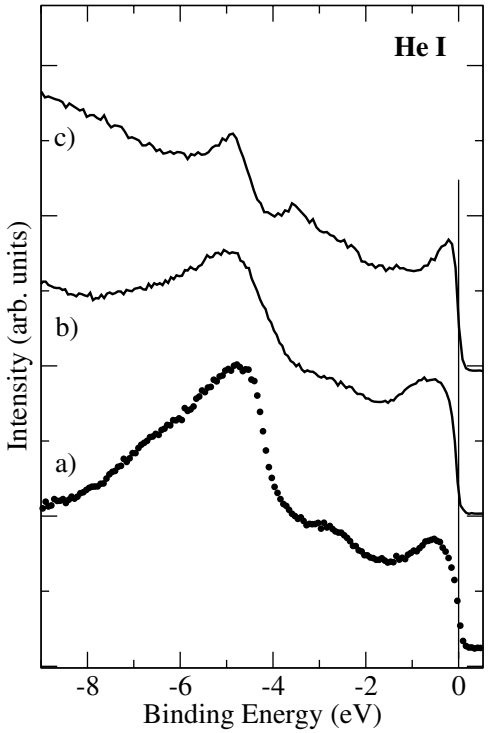

Figure 8. Valence bands for a nitrided Fe(001) sample after annealing at 680 K (a) compared to the Fe(001) single crystal with 0.5 ML of N (b) and a thin film of Fe_4N growth on Cu(001) (c).

γ''-FeN film grown on Cu(001). In this case, the iron nitride evolves to Fe_4N [10] after annealing. This different behavior can be explained, considering that the nitrogen atoms have a different diffusion coefficient in the iron substrate from that in the Cu substrate. Thus, when the FeN is grown on Fe(001), the result of this annealing process is the decomposition of the nitride, eliminating part of the N coming out from the decomposition.

The same thermal evolution behavior is also reflected in the electronic structure of the system. Figures 2(c) and 1(c) show, respectively, the Fe 2p and the N 1s XPS core level peaks for the γ''-FeN thin film after annealing at 680 K. Both curves are identical to that of the initial Fe(001) substrate (figures 2(a) and 1(a)). This disappearance of the N could be explained as due to the high diffusion coefficient of the N in the Fe bulk. When the temperature increases and the γ''-FeN decomposes, the N can either become diffused in the iron bulk or become desorbed from the surface [2], so that only half a monolayer in the $c(2 \times 2)$ structure on Fe remains. The latter structure can be observed by UPS (figure 8(a)) or by LEED. Summarizing, the diffusion of the nitrogen atoms into the Fe bulk hinders the formation of other iron nitride phases, which are more stable at high temperatures (i.e. Fe_4N).

It is important to note that Wit *et al* [37] have already shown that N diffused readily into bulk Fe, even at temperatures as low as 420 K. In our work we have observed that, even at room temperature, there is a strong diffusion of atomic nitrogen in Fe(001), resulting in the nitridation of the surface.

4. Conclusions

We have shown that, by exposing a bcc Fe(001) single crystal to an atomic N plasma at room temperature, a well-characterized ZB iron nitride film of 30 Å thickness is formed. This phase formation implies an easy diffusion of the N atoms in the Fe(001) bulk. Our results confirm previous works [2, 35, 36] that indicate that the rate-limiting step in the nitrogen diffusion of the molecular N_2 is the dissociative chemisorption of nitrogen on the iron surface. The thermal annealing of the system transforms the FeN film into Fe metal, stressing the conclusion that the Fe(001) single crystal surface is not a barrier for the diffusion of N atoms.

As a consequence of the high diffusion coefficient, the N atoms placed at the subsurface facilitate the growth of the γ''-FeN, which appears to be the thermodynamically stable phase at room temperature [10]. Although this phase formation implies a very large adsorption-induced relaxation of the iron (001) planes, the system is stable, as our experimental results indicate and the first-principle calculations support.

The formation of iron nitride overlayers at the iron surface is of technological interest because it improves surface mechanical and anticorrosive properties [38, 39]. Although the iron nitride formed phase is paramagnetic, the metallic behavior of the phase makes the system appealing on spintronic, since we have built a ferromagnetic material (Fe) covered by a paramagnetic metal layer (FeN), which is at the base of spin-valve devices. In this case, the metallic film, of nanometer scale, also acts as a protective coating.

Acknowledgments

CN acknowledges support from an FPI fellowship from the Spanish MEC (FP-2001-1310). This work received financial support from MICINN (FIS 2007-61114, CONSOLIDER on Molecular Nanoscience, FP2001-1310 and MAT2004-05865), CM (Nanomagnet program) and EU (under the PF6 'Structuring the European Research Area' program, contract number RII3-CT-2004-506008).

References

[1] Wert C and Zener C 1949 *Phys. Rev.* **76** 1169–75
[2] Bozso F, Ertl G, Grunze M and Weiss M 1977 *J. Catal.* **49** 18
[3] Scholten J J F, Zwietering P, Konvalinka J A and de Boer J H 1959 *Trans. Faraday Soc.* **55** 2166
[4] Ertl G, Grunze M and Weiss M 1976 *J. Vac. Sci. Technol.* **13** 314
[5] Diekmann W, Panzner G and Grabke H J 1989 *Surf. Sci.* **218** 507–18
[6] Mortensen J J, Gandublia-Pirovana M V, Hansen L B, Hammer B and NCrskov J K 1999 *Surf. Sci.* **422** 8
[7] Grabke H J, Paulitschke W, Tauber G and Viefhaus H 1977 *Surf. Sci.* **63** 377
[8] Grunze M, Bozso F, Ertl G and Weiss M 1977 *Appl. Surf. Sci.* **1** 103
[9] Grabke H J and Viefhaus H 1990 Surface segregation of nonmetal atoms on metal surfaces *Surface Segregation and Related Phenomena* ed P A Dowben and A Miller (Boca Raton, FL: CRC Press)
[10] Navío C, Capitán M J, Alvarez J, Yndurain F and Miranda R 2008 *Phys. Rev.* B **78** 155417
[11] Grachev S, Borsa D M, Vongtragool S and Boerma D O 2001 *Surf. Sci.* **482** 802
[12] Navío C, Capitan M J, Alvarez J, Yndurain F and Miranda R 2007 *Phys. Rev.* B **76** 085105
[13] Kohn W and Sham L J 1965 *Phys. Rev.* A **140** 1133
[14] Soler J M, Artacho E, Gale J D, Garcia A, Junquera J, Ordejon P and Sanchez-Portal D 2002 *J. Phys.: Condens. Matter* **14** 2745

[15] Rao C N R and Ranga Rao G 1991 *Surf. Sci. Rep.* **13** 223–63
[16] Navío C, Alvarez J, Capitan M J, Ecija D, Gallego J M, Yndurain F and Miranda R 2007 *Phys. Rev.* B **75** 125422
[17] Uebing C 1998 *Prog. Solid State Chem.* **26** 155–240
[18] Li X, Zhang Z and Henrich V E 1993 *J. Electron Spectrosc. Relat. Phenom.* **63** 253
[19] Imbihl R *et al* 1982 *Surf. Sci.* **123** 129
[20] Pedersen M 2000 *Phys. Rev. Lett.* **84** 4898–901
[21] Nakagawa H, Nasu S, Fujii H, Takahashi M and Kanamaru F 1991 *Hyperfine Interact.* **69** 455
[22] Gupta M, Gupta A, Bhattacharya P, Misra P and Kukraja L M 2001 *J. Alloys Compd.* **326** 265
[23] Rissanen L, Neubauer N, Lieb K P and Schaaf P 1998 *J. Alloys Compd.* **274** 74
[24] Rissanen L, Shaaf P, Neubauer N, Lieb K P, Keinonen J and Sajavaara T 1999 *Appl. Surf. Sci.* **138** 261
[25] Hinomura T and Nasu S 1998 *Hyperfine Interact.* **11** 221
[26] Perdew J P, Burke K and Ernzerhof M 1996 *Phys. Rev. Lett.* **77** 3865
[27] Troullier N and Martins J L 1991 *Phys. Rev.* B **43** 1993
[28] Kleinman L and Bylander D M 1982 *Phys. Rev. Lett.* **48** 1425
[29] Chubb S R and Pickett W E 1987 *Phys. Rev. Lett.* **58** 1248
[30] Blonski P, Kiejna A and Hafner J 2005 *Surf. Sci.* **590** 88
[31] Legg K O, Jona F, Jepsen D W and Marcus P M 1977 *Phys. Rev.* B **16** 5271
[32] Pignocco A J and Pellisier G E 1965 *J. Electrochem. Soc.* **112** 1188
[33] Simmons G W and Dwyer D J 1975 *Surf. Sci.* **48** 373
[34] Brucker C F and Rhodin T N 1976 *Surf. Sci.* **57** 523
[35] Pick S, Legare P and Demangeat C 2007 *Phys. Rev.* B **75** 195446
[36] Panczyk T 2007 *J. Phys. Chem.* C **111** 3175
[37] de Wit L, Weber T, Custer J S and Saris F W 1994 *Phys. Rev. Lett.* **72** 3835–8
[38] Appolaire B and Goune M 2006 *Comput. Mater. Sci.* **38** 126
[39] Luo X and Liu S 2007 *J. Magn. Magn. Mater.* **308** L1